

## Structural characterization of sulphate borophosphate glasses containing calcium oxide

Yamusa Abdullahi Yamusa <sup>a, b, \*</sup>, Rosli Hussin <sup>a</sup>, Wan Nurulhuda Wan Shamsuri <sup>a</sup>, Sadiq Abubakar Dalhatu <sup>a</sup>, Aliyu Mohammed Aliyu <sup>a</sup>, Ibrahim Bulus <sup>a</sup>

<sup>a</sup> Department of Physics, Faculty of Science, Universiti Teknologi Malaysia, 81310 UTM Johor Bahru, Johor, Malaysia

<sup>b</sup> Centre For Energy Research and Training, Ahmadu Bello University, Zaria, Nigeria

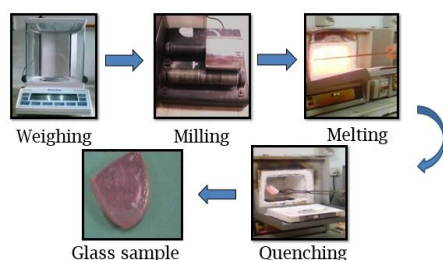
\*Corresponding author: yamusaabdullahi@yahoo.com

### Article history

Received 12 April 2017

Accepted 2 August 2017

### Graphical abstract



### Abstract

Increasing demands for better performing glasses have lead to current investigating of the sturctural properties of glasses for optimum performances. Calcium sulphate borophosphate glasses of different compositions were prepared using melt quenching technique. The glass forming ability and stability were checked using Differential thermal analyzer (DTA). Density and molar volume had been evaluated and analyzed. From the results of XRD, the absnt of discrete and continuous sharp peaks confirmed the amorphous nature of the glass compositions while the results from both IR and Raman revealed the existence of  $\text{SO}_4$ ,  $\text{BO}_4$ ,  $\text{BO}_3$ , P-O-P and  $\text{PO}_4^{3-}$ . Addition of  $\text{CaSO}_4$  to borophosphate influenced the conversion of the dominant  $\text{BO}_3$  groups to  $\text{BO}_4$  groups. The structure of the samples was mainly based on metaphosphate, diphosphate and  $\text{BO}_4$  units, which became depolymerized with addition of  $\text{CaSO}_4$  content. The glass forming ability and thermal stability were found to increase with an increase in the concentration of modifier content. Glass density and molar volume is found to be between 2.146 to 2.314  $\text{gcm}^{-3}$  and 45.794 to 48.880  $\text{m}^3\text{mol}^{-1}$  respectively. It is observed that the density of glass increased while the molar volume also increased with respect to increase in concentration of  $\text{CaSO}_4$  in the glass compositions. We analysed our data using different mechanisms and compared the results with previous works. Our findings show that this glass could be beneficial and considered as a good candidate for optical devices applications.

**Keywords:** Sulphate borophosphate glass, x-ray diffraction, differential thermal analyser, infrared and raman spectroscopy

© 2017 Penerbit UTM Press. All rights reserved

## INTRODUCTION

Borophosphate based glasses have remained the focus of numerous studies due to their unique features for diversity of applications (Karabulut et al., 2015). Glasses containing  $\text{B}_2\text{O}_3$  are of predominant used as non-linear photonic materials and as laser hosts having high optical parameters (Srinivasulu et al., 2013). However, unlike silicate and phosphate - based glasses, little studies have been done on borophosphate-glasses. The structural studies of borophosphate network are inspired by way of the enhancement of the glass properties. The role performed with the aid of  $\text{P}_2\text{O}_5$  and  $\text{B}_2\text{O}_3$  within the glass structure, and the interplay with other factors within the glass network is a motivating subject of glass technology (Pang et al., 2014). These changes in the network structure of borophosphate glasses can be sensitively detected from the changes in Raman spectra of the borophosphate glasses (Vosejpková et al., 2012). Subsequently, the mixture of the two network formers,  $\text{B}_2\text{O}_3$  and  $\text{P}_2\text{O}_5$  allows substantial modifications of the structural and optical properties of the materials compare to simple phosphate and borate host alone (Pang et al., 2014). For instance, the chemical durability can be increased or volume nucleation can be controlled by mixing the phosphate and borate groups. The replacement of alkali oxide with alkaline earth oxide

enhances the strength of cross-linking in the glass structure (Edathazhe and Shashikala, 2016). In these glasses the basic units of pure borate glasses are trigonal  $\text{BO}_3$  groups, whereas those of pure phosphate glasses are  $\text{PO}_4$  tetrahedra linked through covalent bridging oxygen's. The addition of a modifier in some concentration ranges increases the degree of polymerization, the boron coordination changes from trigonal ( $\text{BO}_3$ ) to tetrahedral ( $\text{BO}_4$ ), whereas in phosphate network, an ultra-phosphate network consisting of  $\text{Q}^2$  and  $\text{Q}^3$  tetrahedral (Kumar et al., 2012a).

In this present study sulphate borophosphate glasses contains calcium oxide was analyzed by melt quenching technique and the structural features of the glasses were determined using X-ray diffraction, Thermal differential analyzer, Fourier transformed infrared and Raman spectroscopy.

## EXPERIMENTAL

### Materials

The raw materials used for this study were  $\text{CaSO}_4$  (99.9 % purity),  $\text{B}_2\text{O}_3$  (99.9% purity) and  $\text{P}_2\text{O}_5$  (99.9% purity). Glasses in the  $x\text{CaSO}_4 - 30\text{B}_2\text{O}_3 - (70-x)\text{P}_2\text{O}_5$  with  $15 \leq x \leq 35$  mol % system was prepared by melt quenching technique. The homogenized samples mixture was

poured into alumina crucible. The samples were pre-heated in an electric furnace at 300 °C for 30 minutes and then further heated at 1300 °C for 1h. The melts glass samples were poured onto a brass plate and annealed at 400 °C for about 3hours to remove any internal stresses. Then, samples were allowed to cooled to room temperature. Amorphous nature of the glasses was investigated using a Bruker D8 advance diffractometer with Cu – K $\alpha$  radiations ( $\lambda = 1.54\text{\AA}$ ) operated at 40kv and 100mA. The powder diffraction patterns were recorded on sample in the range of  $2\theta = 10^\circ$ – $100^\circ$  at scanning rate of  $0.05^\circ/\text{s}$ .

The density ( $\rho$ ) of each sample with an error of  $\pm 0.001 \text{ g cm}^{-3}$  was measured using Archimedes principle (Analytical balance of specific density-PrecisaXT220A) with toluene ( $\rho_x = 0.866 \text{ g cm}^{-3}$ ) as the immersion liquid. The density of each sample is determined by the relation  $\rho = \frac{W_a}{W_a - W_b} \rho_x$  where  $W_a$  and  $W_b$  are the sample weight in

air and toluene respectively. The molar volume  $V_m$  is calculated from the relation  $V_m = \frac{M_{av}}{\rho}$

Thermal properties of the glasses were checked using differential thermal analyzer of Perkin Elmer DTA-7 model. A sample of 11mg in powder form was heated at  $10^\circ \text{C/min}$ . The machine operated under a dry nitrogen atmosphere with flow rate of about 200 ml/min. The Hruby parameter  $H$  is used to estimate the stability of the prepared glasses from the relation  $H_g = \frac{T_c - T_g}{T_m - T_c}$

Fourier transform infrared transmissions spectra were recorded in the spectral range of  $400$  to  $3500 \text{ cm}^{-1}$  with Perkin Elmer FTIR 1660 spectrometer. Transparent pellets of each sample were formed by mixing a relatively fine glass powder with KBr at ratio 1:100.

Raman spectrum was obtained using a confocal Horiba Jobin Yvon (Model HR800 UV) in the range of  $400 - 1500 \text{ cm}^{-1}$ . Argon ion laser was used as radiation source with excitation wavelength of  $514.55 \text{ nm}$  and power of  $5 \text{ mW}$ .

## RESULTS AND DISCUSSION

### X- Ray Diffraction

Fig. 1 shows the X-ray diffraction patterns of the prepared borophosphate glasses recorded in the range of  $10^\circ$  to  $100^\circ$ . The results obtained showed that the X-ray diffraction patterns of the sample exhibited broad diffusion at lower scattering angles around  $15$ – $25$  degree. It indicated the presence of long range structural disorder and absence of any sharp peak. This result confirms that the prepared samples are completely amorphous.

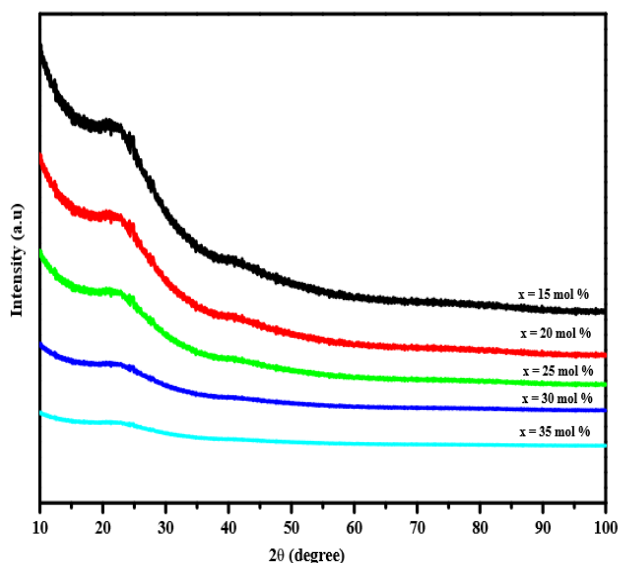


**Fig.1** X-ray diffraction of  $x\text{CaSO}_4 - 30\text{B}_2\text{O}_3 - (70-x)\text{P}_2\text{O}_5$  with  $15 \leq x \leq 35 \text{ mol } \%$ .

### Density and Molar volume measurements

Fig. 2 depicts the variation of  $\text{CaSO}_4$  concentration plotted against density and molar volume of borophosphate glasses. The density and molar volume increases with increasing concentration of  $\text{CaSO}_4$  which indicate an increase of glass network rigidity as shown in Table 1. The increase in the glass density is due to an increase in the number of bridging oxygen in the glass (Arunkumar and Marimuthu, 2013). Furthermore, the increase in molar volume results in an increase in inter-atomic spacing or the bond length (Tanko et al., 2016).

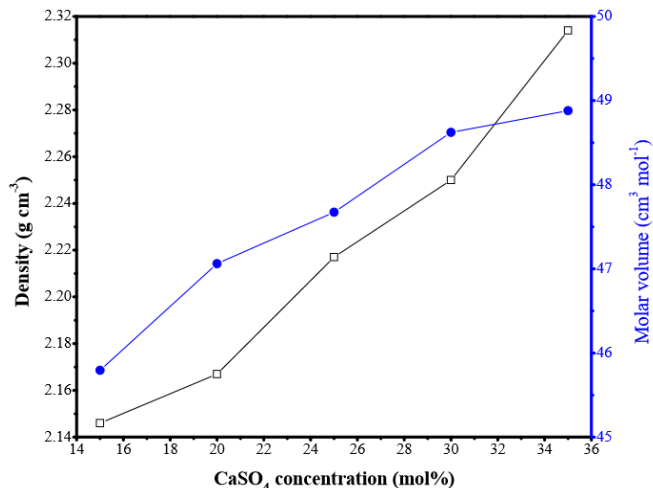


**Fig. 2**  $\text{CaSO}_4$  concentration dependent variation of glass density and molar volume.

**Table 1** Nominal composition of  $x\text{CaSO}_4 - 30\text{B}_2\text{O}_3 - (70-x)\text{P}_2\text{O}_5$  with  $15 \leq x \leq 35 \text{ mol } \%$ , density and molar volume of glasses.

Glass code	$x\text{CaSO}_4$ mol %	(70-x) $\text{P}_2\text{O}_5$ mol %	30 $\text{B}_2\text{O}_3$ mol %	$\rho$ (g cm <sup>-3</sup> )	$V_m$ (cm <sup>3</sup> mol <sup>-1</sup> )
SBP1	15	55	30	2.147	45.794
SBP2	20	50	30	2.167	47.062
SBP3	25	45	30	2.217	47.673
SBP4	30	40	30	2.250	48.622
SBP5	35	35	30	2.314	48.880

### Infrared Spectra

The results of the vibrational spectroscopy of IR gives useful structural information about the short and intermediate range in the glass structure (Stefan and Karabulut, 2014, Wan et al., 2014). In general, the main vibrational modes characteristic of atoms in the glass network are observed in the mid- IR region and these modes are independent of the other groups that may be in the glass structure (Ouis et al., 2012). Since the components investigated in this study consist of two main glass formers in different quantities, we expect to detect vibrational modes belonging to both borate and phosphate groups in the IR spectra. The IR spectra of the glasses studied in the range  $400 - 3500 \text{ cm}^{-1}$  frequency as shown in Fig.3. The strong band observed at  $518$  to  $531 \text{ cm}^{-1}$  assigned to bending mode of  $\text{PO}_4^{3-}$  (Karabulut et al., 2015), the band increased with increasing concentration of  $\text{CaSO}_4$ . Bending of B-O-B linkages of borate network and symmetric bending P-O-P of phosphate is around band at  $735$ – $749 \text{ cm}^{-1}$  (Saitoh et al., 2015) and band at  $850$ – $889 \text{ cm}^{-1}$  are assigned to the asymmetric stretching modes of the in-chain P-O-P linkages (P-O-P)<sub>as</sub> (Kumar et al., 2012b). The band at  $1049$ – $1071 \text{ cm}^{-1}$  are a mixture from  $\nu(\text{SO}_4)$  and  $\nu(\text{BO}_4)$  (Daub et al., 2014). The bands at  $1260$ – $1309 \text{ cm}^{-1}$  are assigned to boroxol rings (Rada et al., 2010). The bands around  $1429$ – $1443 \text{ cm}^{-1}$  have been

assigned to the stretching relaxation of the bond between borate trigonal  $\text{BO}_3$  and oxygen units (Leow et al., 2014). Addition of  $\text{CaSO}_4$  to the glass network can alter the glass lattice, open up the network structure, lower the viscosity, weaken the bond strength of the glass and improve the glass stability (Shen et al., 2015). The variation of the spectra is due to the increase in  $\text{CaSO}_4$  content. Therefore, this variation creates larger number of non-bridging oxygen in the glass network. As a consequences of that, the phosphate coordination drastically reduces from 4-fold to 3-fold to 2-fold and even dimensional. Therefore, the depolymerization of P-O-P, and B-O-B take place and strength of the glass decreases (Kumar et al., 2012c). However, it was observed that the IR intensities signifies the increase degree of disorder in the network with increase in concentration of  $\text{CaSO}_4$ . The summary of IR findings and reported values are shown in Table 2.

### Raman Spectra

The Raman spectra of  $x\text{CaSO}_4 - 30\text{B}_2\text{O}_3 - (70-x)\text{P}_2\text{O}_5$  glasses are shown in Fig. 4. The borophosphate glasses reveals one broad vibrational band in the high frequency region with a maximum at  $1420 - 1424 \text{ cm}^{-1}$  is due to the asymmetric stretching vibration of  $\text{BO}_3$  units

(Ganguli and Rao, 1999). The band at  $1359-1361 \text{ cm}^{-1}$  is due to the asymmetric stretching vibration of  $\text{BO}_3$  units (Suresh et al., 2012). The band at  $1170-1179 \text{ cm}^{-1}$  can be ascribed to the symmetric vibration of  $\text{PO}_2$  of metaphosphate  $\text{Q}^2$  (Kim et al., 2010). The band at  $1057 - 1061 \text{ cm}^{-1}$  is due to the symmetric stretching vibration of the tetra hedral  $\text{SO}_4$  and  $\text{BO}_4$  units (Daub et al., 2014). The weak band at  $777-780 \text{ cm}^{-1}$  can be ascribed to the symmetric strength vibration of  $\text{BO}_3$  and  $\text{BO}_4$  groups (Vyatchina et al., 2009). The weak band at  $615-624 \text{ cm}^{-1}$  can be ascribed to the vibrations of oxygen atoms in P-O-P bridges between metaphosphate  $\text{Q}^2$  and diphosphate  $\text{Q}^1$  units (Koudelka et al., 2014). The weak band located at  $480-482 \text{ cm}^{-1}$  can be ascribed to the bending mode vibration of  $\text{SO}_4^{2-}$  (Ganguli and Rao, 1999). It was observed that a prominent and broadening of the band at  $1420-1420 \text{ cm}^{-1}$  is due to the disorder glass structure (Muñoz-Martín, et al, 2009). It was observed that, by increasing the  $\text{CaSO}_4$ , the vibration peaks slightly shifted to higer wavelength up to 35%. This shift could indicate the effect of the  $\text{CaSO}_4$ , thereby, influencing the shape of the network structure and create non-bridging oxygen resulting in the depolymerization of phosphate network (Hoppe, U., et al, 2007). The summary of Raman findings and reported values are shown in Table 3.

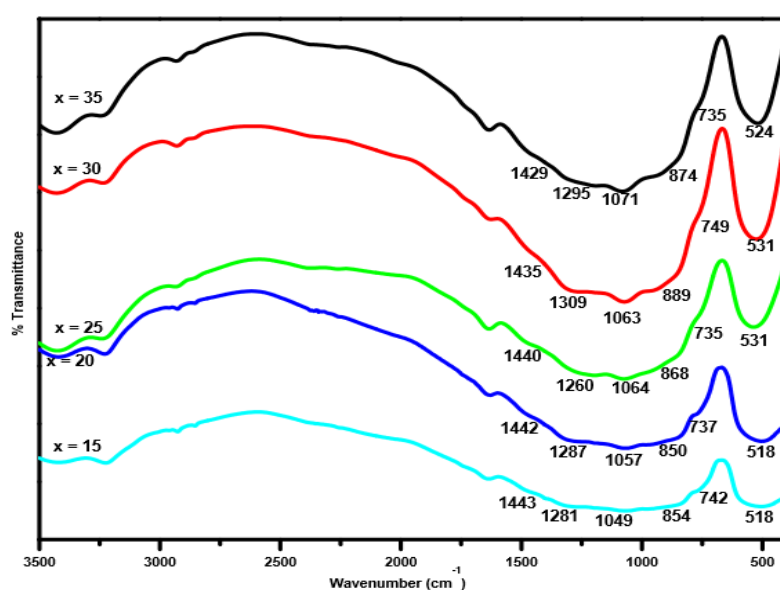


Fig.3 The IR spectra of  $x\text{CaSO}_4 - 30\text{B}_2\text{O}_3 - (70-x)\text{P}_2\text{O}_5$  with  $15 \leq x \leq 35$  mol %.

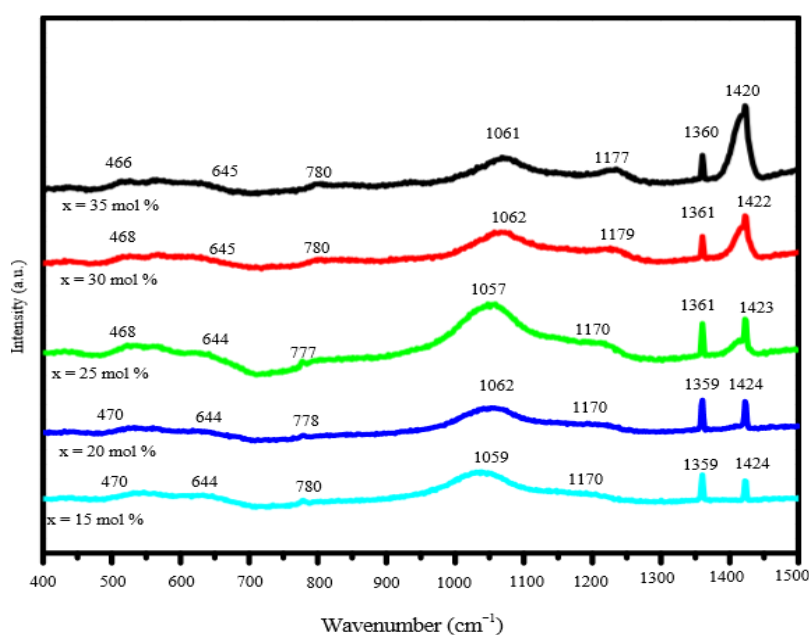


Fig.4 The Raman spectra of  $x\text{CaSO}_4 - 30\text{B}_2\text{O}_3 - (70-x)\text{P}_2\text{O}_5$  with  $15 \leq x \leq 35$  mol

**Table 2** IR band assignment and the reported values for  $x\text{CaSO}_4 - 30\text{B}_2\text{O}_3 - (70-x)\text{P}_2\text{O}_5$  with  $15 \leq x \leq 35$  mol % glasses.

IR Band position in $\text{cm}^{-1}$ with varying conc. of $\text{CaSO}_4$					Reported ( $\text{cm}^{-1}$ )	Assignment
15 (mol%)	20 (mol%)	25 (mol%)	30 (mol%)	35 (mol%)		
518	518	531	531	524	500-580	Bending mode of $\text{PO}_4^{3-}$
742	737	735	749	735	745-760	Stretching vibration of P-O-P
854	850	868	889	874	844-964	Asymmetric vibration of P-O-P
1049	1057	1064	1063	1071	1060-1080	Mixture from $\nu(\text{SO}_4)$ and $\nu(\text{BO}_4)$
1281	1287	1260	1309	1295	1240-1350	Boroxol rings
1443	1442	1440	1435	1429	1400-1450	Stretching vibration of trigonal $\text{BO}_3$

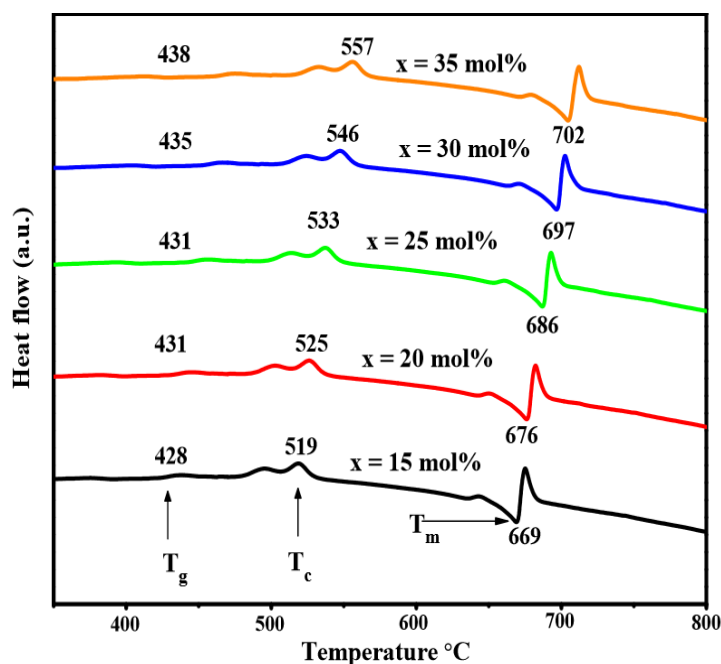
**Table 3** Raman band assignment and the reported values for  $x\text{CaSO}_4 - 30\text{B}_2\text{O}_3 - (70-x)\text{P}_2\text{O}_5$  with  $15 \leq x \leq 35$  mol % glasses.

Raman Band position in $\text{cm}^{-1}$ with varying conc. of $\text{CaSO}_4$					Reported ( $\text{cm}^{-1}$ )	Assignment
15 mol %	20 mol%	25 mol%	30 mol%	35 mol%		
470	470	468	468	466	465	Bending mode vibration of $\text{SO}_4^{2-}$
644	644	644	645	645	645	P-O-P bridges between metaphosphate $\text{Q}^2$ and diphosphate $\text{Q}^1$ units
780	778	777	780	780	720-780	Symmetric strength vibration of $\text{BO}_3$ and $\text{BO}_4$ groups
1059	1062	1057	1062	1061	1060	Symmetric stretching vibration of the tetra hedral $\text{SO}_4$ and $\text{BO}_4$ units
1170	1170	1170	1179	1170	1165-1180	Symmetric vibration of $\text{PO}_2$ of metaphosphate $\text{Q}^2$
1359	1359	1361	1361	1360	1200 -1400	Asymmetric stretching vibration of $\text{BO}_3$ units
1424	1424	1423	1422	1429	1420 -1485	Asymmetric stretching vibration of $\text{BO}_3$ units

### Thermal Differential Analysis

The results of DTA measurements are shown in Fig. 5. The sharp endothermic peak is corresponding to the melting temperature ( $T_m$ ) at  $669-702^\circ\text{C}$ , the exothermic peak is corresponding to the crystallization temperature ( $T_c$ ) at  $519-557^\circ\text{C}$  and the tiny peak is corresponding to the glass transition temperature ( $T_g$ ) at  $428-438^\circ\text{C}$  (Gilbert, J. C. & Nosedal, J. 1992). Both the glass transition temperature and the crystallization temperature increases with an increasing  $\text{CaSO}_4$  content. Table 4 displays the values of  $T_g$ ,  $T_c$  and  $T_m$  and calculated glass

stability (S) and Hruby parameter for the borophosphate glasses. It was observed that the thermal analysis depicts an increase of glass transition due to the addition of  $\text{B}_2\text{O}_3$ . This is an indication that combining  $\text{P}_2\text{O}_5$  and  $\text{B}_2\text{O}_3$  improves the strength of the host. The thermal Hruby parameters of SBP1 and SBP2 has been observed to be 0.6067 and 0.6225. This falls around the limit of thermal Hruby of 0.5 as reported by (Alajerami et al., 2012). This shows that samples SBP1 and SBP2 could be considered as the best glass former with good thermal stability among the prepared samples.

**Fig. 5** The DTA spectra of  $x\text{CaSO}_4 - 30\text{B}_2\text{O}_3 - (70-x)\text{P}_2\text{O}_5$  with  $15 \leq x \leq 35$  mol %.

**Table 4** CaSO<sub>4</sub> concentration dependent thermal properties of the prepared glasses.

Glass code	T <sub>g</sub> (°C)	T <sub>c</sub> (°C)	T <sub>m</sub> (°C)	S = T <sub>c</sub> - T <sub>g</sub> (°C)	H
SBP1	428	519	669	91	0.6067
SBP2	431	525	676	94	0.6225
SBP3	431	533	686	102	0.6666
SBP4	435	546	697	111	0.7350
SBP5	438	557	702	119	0.7986

## CONCLUSIONS

The structural properties of sulphate borophosphate glasses containing calcium oxide were investigated in the range  $x\text{CaSO}_4 - 30\text{B}_2\text{O}_3 - (70-x)\text{P}_2\text{O}_5$  with  $15 \leq x \leq 35$  mol % composition line. The amorphous nature of the glass is confirmed by XRD analysis. The IR spectra of these glasses show the existence of  $\text{BO}_3$ ,  $\text{BO}_4$ ,  $\text{PO}_4^{3-}$ , P-O-P and  $\text{SO}_4$ . The IR and Raman studies indicated that the increase of CaSO<sub>4</sub> content influence significant effect of the network structure and create non-bridging oxygen. Raman spectroscopy describe the structural formation changes of stable boron and phosphorus oxygen groups with characteristics of metaphosphate and diphosphate groups. The thermal properties of sulphate borophosphate glasses such as the transition temperature, crystallisation temperature, stability and glass forming ability are determined from DTA analysis and found to be thermally stable. The stability factor (S) is found in the range of 91 – 119 °C which indicates an increasing stability with addition of CaSO<sub>4</sub> concentration. It is found that sample SBP1 and SBP2 have good glass forming ability and stability among the prepared glass samples. Glass density and molar volume is found to be between 2.146 to 2.314 gcm<sup>-3</sup> and 45.794 to 48.880 m<sup>3</sup>mol<sup>-1</sup> respectively. The obtained findings may provide some useful information towards the development of sulphate borophosphate glasses based solid state lasers.

## ACKNOWLEDGEMENT

We are thankful to the Ministry of Higher Education Malaysia and UTM for given us financial assistance through the fundamental research grant scheme (FRGS), vote number (QJ130000.2526.10H01).

## REFERENCES

- Alajerami, Y. S. M., Hashim, S., Hassan, W. M. S. W. and Ramli, A. T. 2012. The effect of titanium oxide on the optical properties of lithium potassium borate glass. *Journal of Molecular Structure*, 1026, 159-167.
- Arunkumar, S., Marimuthu, K. 2013. Concentration effect of  $\text{Sm}^{3+}$  ions in  $\text{B}_2\text{O}_3\text{-PbO-PbF}_2\text{-Bi}_2\text{O}_3\text{-ZnO}$  glasses—structural and luminescence investigations. *Journal of Alloys and Compounds*, 565, 104-114.
- Daub, M., Höpfe, H. A. & Hillebrecht, H. 2014. Further new borosulfates: synthesis, crystal structure, and vibrational spectra of  $\text{A}[\text{B}(\text{SO}_4)_2](\text{A} = \text{Na}, \text{K}, \text{NH}_4)$  and the crystal structures of  $\text{Li}_5[\text{B}(\text{SO}_4)_4]$  and  $\text{NH}_4[\text{B}(\text{S}_2\text{O}_7)_2]$ . *Zeitschrift für Anorganische und Allgemeine Chemie*, 640, 2914-2921.
- Edathazhe, A. B., Shashikala, H. 2016. Effect of BaO addition on the structural and mechanical properties of soda lime phosphate glasses. *Materials Chemistry and Physics*, 184, 146-154.
- Ganguli, M., Rao, K. 1999. Studies on the effect of  $\text{Li}_2\text{SO}_4$  on the structure of lithium borate glasses. *The Journal of Physical Chemistry B*, 103, 920-930.
- Gilbert, J. C., Nocedal, J. 1992. Global convergence properties of conjugate gradient methods for optimization. *SIAM Journal on Optimization*, 2, 21-42.
- Hoppe, U., Brow, R. K., Tischendorf, B. C., Kriltz, A., Jónvári, P., Schöps, Hannon, A. C., 2007. Structure of titanophosphate glasses studied by X-ray and neutron diffraction. *Journal of Non-Crystalline Solids*, 353(18), 1802-1807.
- Karabulut, M., Popa, A., Borodi, G., Stefan, R. 2015. An FTIR and ESR study of iron doped calcium borophosphate glass-ceramics. *Journal of Molecular Structure*, 1101, 170-175.
- Kim, N.-J., Im, S.-H., Kim, D.-H., Yoon, D.-K., Ryu, B.-K. 2010. Structure and properties of borophosphate glasses. *Electronic Materials Letters*, 6, 103-106.
- Koudelka, L., Rösslerová, I., Černošek, Z., Mošner, P., Montagne, L., Revel, B. 2014. The structural role of tellurium dioxide in lead borophosphate glasses. *Journal of Non-Crystalline Solids*, 401, 124-128.
- Kumar, A. R., Rao, C. S., Krishna, G. M., Kumar, V. R., Veeraiah, N. 2012a. Structural features of  $\text{MoO}_3$  doped sodium sulpho borophosphate glasses by means of spectroscopic and dielectric dispersion studies. *Journal of Molecular Structure*, 1016, 39-46.
- Kumar, A. R., Rao, C. S., Rao, N. N., Kumar, V. R., Kityk, I., Veeraiah, N. 2012b. Influence of valence and coordination of manganese ions on spectral and dielectric features of  $\text{Na}_2\text{SO}_4\text{-B}_2\text{O}_3\text{-P}_2\text{O}_5$  glasses. *Journal of Non-Crystalline Solids*, 358, 1278-1286.
- Kumar, A.R., Rao, C.S., Srikumar, T., Gandhi, Y., Kumar, V.R., Veeraiah, N., 2012. Dielectric dispersion and spectroscopic investigations on  $\text{Na}_2\text{SO}_4\text{-B}_2\text{O}_3\text{-P}_2\text{O}_5$  glasses mixed with low concentrations of  $\text{TiO}_2$ . *Journal of Alloys and Compounds*, 515, pp.134-142.
- Leow, T., Leong, P., Eeu, T., Ibrahim, Z., Hussin, R. 2014. Study of structural and luminescence properties of lead lithium borophosphate glass system doped with Ti ions. *Sains Malaysiana*, 43, 929-934.
- Muñoz-Martín, D., Villegas, M. A., Gonzalo, J., Fernández-Navarro, J. M., 2009. Characterisation of glasses in the  $\text{TeO}_2\text{-WO}_3\text{-PbO}$  system. *Journal of the European Ceramic Society*, 29(14), 2903-2913.
- Ouis, M. A., Abdelghany, A. M., Elbatal, H. A. 2012. Corrosion mechanism and bioactivity of borate glasses analogue to Hench's bioglass. *Processing and Application of Ceramics*, 6, 141-149.
- Pang, X. G., Eeu, T. Y., Leong, P. M., Shamsuri, W., Nurulhuda, W., Hussin, R. Structural and luminescence study of rare earth and transition metal ions doped lead zinc borophosphate glasses. *Advanced Materials Research*, 2014. Trans Tech Publ, 280-283.
- Rada, M., Rada, S., Pascuta, P., Culea, E. 2010. Structural properties of molybdenum-lead-borate glasses. *Spectrochimica Acta Part A: Molecular and Biomolecular Spectroscopy*, 77, 832-837.
- Saitoh, A., Tricot, G., Rajbhandari, P., Anan, S., Takebe, H. 2015. Effect of  $\text{B}_2\text{O}_3/\text{P}_2\text{O}_5$  substitution on the properties and structure of tin boro-phosphate glasses. *Materials Chemistry and Physics*, 149, 648-656.
- Srinivasulu, K., Omkaram, I., Obeid, H., Kumar, A. S., Rao, J. 2013. Structural and magnetic properties of  $\text{Gd}^{3+}$  ions in sodium-lead borophosphate glasses. *Journal of Molecular Structure*, 1036, 63-70.
- Stefan, R., Karabulut, M. 2014. Structural properties of iron containing calcium-magnesium borophosphate glasses. *Journal of Molecular Structure*, 1071, 45-51.
- Suresh, S., Pavani, P. G., Mouli, V. C. 2012. ESR, optical absorption, IR and Raman studies of  $x\text{TeO}_2 + (70-x)\text{B}_2\text{O}_3 + 5\text{TiO}_2 + 24\text{R}_2\text{O} : 1\text{CuO}$  ( $x = 10, 35$  and  $60\text{mol}\%$ ;  $\text{R} = \text{Li}, \text{Na}$  and  $\text{K}$ ) quaternary glass system. *Materials Research Bulletin*, 47, 724-731.
- Shen, L. F., Chen, B. J., Pun, E. Y. B., Lin, H. 2015.  $\text{Sm}^{3+}$ -doped alkaline earth borate glasses as  $\text{UV} \rightarrow \text{visible}$  photon conversion layer for solar cells. *Journal of Luminescence*, 160, 138-144.
- Tanko, Y., Sahar, M., Ghoshal, S. 2016. Prominent spectral features of  $\text{Sm}^{3+}$  ion in disordered zinc tellurite glass. *Results in Physics*, 6, 7-11.
- Vosejpková, K., Koudelka, L., Černošek, Z., Mošner, P., Montagne, L., Revel, B. 2012. Structural studies of boron and tellurium coordination in zinc borophosphate glasses by  $^{11}\text{B}$  MAS NMR and Raman spectroscopy. *Journal of Physics and Chemistry of Solids*, 73, 324-329.
- Vyatchina, V., Perelyaeva, L., Zuev, M., Baklanova, I. 2009. Structure and properties of glasses in the  $\text{MgSO}_4\text{-Na}_2\text{B}_4\text{O}_7\text{-KPO}_3$  system. *Glass Physics and Chemistry*, 35, 580-585.
- Wan, M. H., Wong, P. S., Hussin, R., Lintang, H. O., Endud, S. 2014. Structural and luminescence properties of  $\text{Mn}^{2+}$  ions doped calcium zinc borophosphate glasses. *Journal of Alloys and Compounds*, 595, 39-45.